



Cite this: *RSC Adv.*, 2020, 10, 33517

Preactivated-thiolated polyacrylic acid/1-vinyl pyrrolidone nanoparticles as nicotine carriers for smoking cessation

Chaikarn Pornpitchanarong, Theerasak Rojanarata, Praneet Opanasopit, Tanasait Ngawhirunpat and Prasopchai Patrojanasophon *

This study aimed to develop nicotine-loaded mucoadhesive preactivated-thiolated polymeric nanoparticles (PNPs) for smoking cessation. 2-Mercaptonicotinic acid (2MNA) was coupled as dithionicotinic acid dimer and used in the preactivation of thiolated polyacrylic acid/vinyl pyrrolidone PNPs (thiolated AA/VP PNPs). Preactivated-thiolated AA/VP PNPs were synthesized through surfactant-free emulsion polymerization and coupling reactions. The structural attributes of the preactivated-thiolated AA/VP PNPs were characterized using Fourier-transform infrared spectroscopy and proton nuclear magnetic resonance spectroscopy. The particle size and zeta potential were evaluated by dynamic light scattering evaluation. The morphology of the preactivated-thiolated AA/VP PNPs was examined using scanning electron microscopy. In addition, the mucoadhesive properties, drug loading and release, and biocompatibility of the preactivated-thiolated AA/VP PNPs were assessed. The spherical preactivated-thiolated AA/VP PNPs were successfully synthesized with a particle size of 410.3 ± 7.4 nm and a negative surface charge. The preactivated-thiolated AA/VP PNPs exhibited superior mucoadhesive properties compared with the thiolated AA/VP PNPs. Drug loading by PNP to a nicotine ratio of 1 : 1 provided desirable loading capacity and % loading efficiency of 285.7 ± 36.7 $\mu\text{g mg}^{-1}$ and $57.1 \pm 7.4\%$, respectively. More than 50% of the nicotine contained in the PNPs was rapidly released in the first hour, followed by a sustained release for up to 12 h. Moreover, the synthesized PNPs were non-toxic to human gingival cells. Therefore, the preactivated-thiolated AA/VP PNPs may be a candidate carrier of nicotine for smoking cessation.

Received 10th July 2020
Accepted 4th September 2020

DOI: 10.1039/d0ra06039a

rsc.li/rsc-advances

Introduction

Cigarette smoking is a major cause of preventable death in the world today. The use of tobacco leads to chronic diseases and complications, including chronic obstructive pulmonary disease, asthma, atherosclerotic cardiovascular disease, and lung cancer.¹ Nicotine is a euphoriant addictive compound in cigarettes; it modulates the release of dopamine and other neurotransmitters, affecting the moods and pleasures of smokers. However, nicotine withdrawal symptoms of depression, irritability, anxiety, and restlessness also cause addiction and smoking urge leading to unsuccessful smoking cessation.^{2,3} Behavioural modification, tapering off, non-nicotine pharmacotherapy, and nicotine replacement therapy (NRT) may be employed as strategies for smoking cessation.⁴

NRTs play an essential role in smoking cessation.^{5–7} The use of NRT reduces the withdrawal symptoms, and appropriate doses should be used to reduce addiction to cigarette nicotine.⁸

Commercially available nicotine for smoking cessations consist of gums, transdermal patches, tablets, nasal sprays, oral inhalers, and film strips. Examples of the marketed products include Nicotinnell®, Nicorette® (gums and patches), and NiQuitin® strips, which play a significant role in the current NRT for the immediate and prolonged delivery of nicotine. Apart from the transdermal patches that can prolong nicotine release, other formulations offer an acute relief of nicotine or tobacco craving.⁹ Short-acting formulations of NRTs may need dose titration, frequent dosing, and possess a high risk of relapse, whereas long-acting patches can cause skin irritation and sleep disturbance.¹⁰ Novel nicotine preparations are being developed to enhance smokers' compliances, improve drug pharmacokinetics, and increase the quitting rate. The development of new nicotine formulations, such as mouth spray, drops/straw, films, freeze-dried wafers, and more advanced creations, has been investigated.^{11–14} Mucoadhesive drug delivery refers to a system that can adhere to the mucosal lining and provide prolonged residence time, localized delivery, fast action, and increased bioavailability.^{15,16} Mucoadhesive drug delivery systems can be employed in the delivery of nicotine for smoking cessation as the formulation can adhere to the oral mucosa, and release nicotine in a controllable approach, thus

Pharmaceutical Development of Green Innovations Group (PDGIG), Faculty of Pharmacy, Silpakorn University, Nakhon Pathom, 73000, Thailand. E-mail: patrojanasophon_p@su.ac.th



reducing the smokers' dependency on smoking.¹⁵ First-generation mucoadhesive materials (such as chitosan, alginate, and methylcellulose) adhere to the mucous membrane through weak bonds (physical entanglement, hydrogen bond, van der Waals force, and ionic interactions). On the other hand, the second-generation mucoadhesive polymers can form a strong covalent bond with the mucin glycoprotein.¹⁷ Thiomers or thiolated polymers are well-known as new generation mucoadhesive polymers that can form disulfide linkage with the cysteine-rich domain in the mucin glycoprotein. They enhance penetration across the mucosal surface, leading to increased bioavailability.^{18,19} Given the drawbacks of conventional thiomers, including the generation of thiol oxidation and disulfide exchange, preactivated-thiomers were invented to resolve such issues.²⁰ Formerly, a study reported the S-protected hyaluronic acid derived from polymer thiolation with mercaptanotinic acid (MNA). S-Preactivated L-cysteine is stable in an oxidative environment and provides high viscosity and improved mucoadhesive property on the intestinal and a conjunctival mucosal membrane.²¹

Polymeric nanoparticles (PNPs) offer various benefits in drug delivery. The colloidal systems of PNPs having a particle size of less than 1000 nm exhibit an extensive surface area and provide high drug-loading and controlled-release profile, which render the PNPs attractive for drug delivery.^{22,23} To improve nicotine delivery compared with the commercially available nicotine formulations, *e.g.*, nicotine gum, the development of mucoadhesive PNPs may be advantageous by prolonging the adhesion time of nicotine carrier on the oromucosal surface and extend the delivery duration of nicotine which may benefit the prevention of frequent nicotine craving and avoid withdrawal symptoms. Mucoadhesive PNPs can be further formulated as oral spray preparations to ease the use of products for cigarette quitters. Herein, we report the synthesis of mucoadhesive preactivated-thiolated PNPs as nicotine carriers for smoking cessation. The PNPs were synthesized in accordance with our previous study using acrylic acid (AA) and 1-vinyl-2-pyrrolidone (VP) as monomers for the synthesis reaction.²⁴ Then, the PNPs were conjugated with thiol groups and preactivated with 2MNA. VP is a hydrophilic monomer and commonly acquired as a PNP stabilizer. When polymerized, VP helps to avoid particle aggregation through its steric hindrance structure. VP also acts as a dispersant of polymers or PNPs. Importantly, this compound is remarkably stable, inert, and safe.²⁵ AA is a monomer with hydrophilic and biocompatible properties. Its structure contains a carboxylic acid group that can be extensively used to obtain a polymer with various advantages.^{26,27} The structural and physicochemical characteristics, together with the mucoadhesive property, nicotine loading and release, and biocompatibility of the synthesized preactivated-thiolated polyacrylic acid/VP PNPs (preactivated-thiolated AA/VP PNPs) were studied.

Materials and methods

Materials

VP, AA, 2MNA, *N,N'*-methylenebisacrylamide (MBA), 2,2'-azobis(2-methylpropionamide) dihydrochloride (AAPH), L-cysteine hydrochloride, methylthiazolyldiphenyl tetrazolium

bromide (MTT), sodium fluorescein, 5,5'-dithiobis(2-nitrobenzoic acid) (Ellman's reagent), *N*-ethyl-*N'*-(3-dimethylaminopropyl)carbodiimide hydrochloride (EDAC), and *N*-hydroxysuccinimide (NHS) were acquired from Sigma Chemicals (St. Louis, MO, USA). Nicotine was bought from Tokyo Chemical Industry (Chuo-ku, Tokyo, Japan). Other chemicals and reagents were used as purchased without further purification.

Synthesis of preactivated-thiolated AA/VP PNPs

The synthesis of preactivated-thiolated AA/VP PNPs was performed in accordance with the scheme in Fig. 1, with the methods as follows:

Synthesis of AA/VP PNPs

The AA/VP PNPs were synthesized following the method from our previous study with modification.²⁸ Roughly, 0.1% wt AAPH (the initiator) was dissolved in deionized water (100 mL) in a round-bottomed flask heated at 65–70 °C. The synthesis atmosphere was made inert with nitrogen purge. VP and AA (1 : 3 by mole) and 10% wt MBA were dissolved in ethyl acetate (5 mL). The organic mixture was added dropwise to the initiated solution, and the reaction was continued for 18 h. The unreacted monomers and other residues were removed *via* dialysis (molecular weight cut-off 3500 Da) against deionized water for 72 h with water replacement every 6 h. The synthesized product was collected after lyophilization. The synthesized AA/VP PNPs were then characterized using proton nuclear magnetic resonance spectroscopy (¹H-NMR), Fourier-transform infrared spectroscopy (FTIR), carboxylic acid content, particle size, and surface charge.

Synthesis of thiolated AA/VP PNPs

The carbodiimide coupling reaction was performed to obtain the thiolated AA/VP PNPs. Precisely, the AA/VP PNPs were dispersed in deionized water containing EDAC and NHS at the

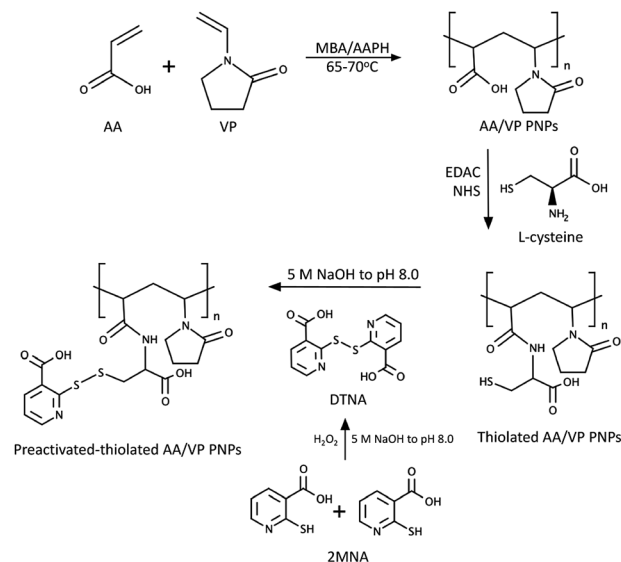


Fig. 1 Synthesis scheme of the 2MNA-SH-AA/VP PNPs.



equivalent mole to L-cysteine and continuously stirred for at least 20 min. The inert environment was achieved by nitrogen flush. Excess amount of L-cysteine (by mole) to the COOH content of the AA/VP PNPs was then added to the reaction, and the reaction mixture was stirred overnight at room temperature. Purification was accomplished by a 3 day dialysis followed by lyophilization. $^1\text{H-NMR}$, FTIR, particle size, and zeta potential of the synthesized PNPs were then investigated.

Synthesis of preactivated-thiolated AA/VP PNPs

The preactivated-thiolated AA/VP PNPs were synthesized using the thiol-disulfide exchange reaction. First, dimers of dithionicotinic acid (DTNA) were synthesized by oxidative coupling of 2MNA monomers, as described in the literature.²⁹ Then, 2MNA (2 g) was dissolved in deionized water (50 mL) with 1 h sonication, and the pH was adjusted to 8.0 with 5 M NaOH, forming a clear-yellowish solution. Hydrogen peroxide (30% v/v, 2.5 mL) was slowly added to the 2MNA solution, and the pH was maintained at 8.0. Then, DTNA was obtained after freeze drying. Dimer formation was confirmed by comparing the UV spectra of DTNA and 2MNA. Second, thiolated AA/VP PNPs (1 g) were dispersed in water (75 mL), and DTNA (50% wt of PNPs) was added to the colloidal dispersion to perform the thiol-disulfide exchange reaction. The pH was adjusted to 8.0 with 5 M NaOH, and the reaction was left to continue for over 12 h. Dialysis was performed to remove the unreacted dimers followed by a freeze-drying process. The obtained PNPs were then characterized in terms of their molecular structure, physicochemical properties, and potential as mucoadhesive drug carriers.

Characterization of the PNPs

$^1\text{H-NMR}$. Structural elucidations of the synthesized PNPs were carried out by $^1\text{H-NMR}$. The synthesized PNPs were weighed (5 mg) and dispersed in deuterium oxide (D_2O). The analysis was performed under a 300 MHz NMR spectrometer AVANCE III HD (Bruker, Billerica, MA, USA) at 298 K. The spectra were recorded and reported as the chemical shifts (δ) in part per million (ppm) using D_2O as a solvent reference ($\delta = 4.80$ ppm).

Attenuated total reflectance-FTIR (ATR-FTIR). The structures of the functionalized-PNPs were ascertained using ATR-FTIR (Nicolet iS5, Thermo Fisher Scientific, MA, USA). Each sample was placed on top of the diamond crystal, and the investigation was performed at 16 running scans and 4 cm^{-1} resolution. The spectra were collected from 400 to 4000 cm^{-1} .

Particle sizes and surface charge. The particle size and surface charge of the synthesized PNPs were analyzed by a Malvern Zetasizer Nano ZS (Malvern, UK). The PNPs were dispersed in ultrapure water, diluted to 1 : 100, and filtered through $0.45\text{ }\mu\text{m}$ syringe filter before being placed in a 1 cm^3 DTS1070 polystyrene latex folded capillary cell. The measurement was carried out in triplicate at $25\text{ }^\circ\text{C}$.

Morphology. The morphological attributes of the preactivated-thiolated AA/VP PNPs were observed by scanning electron microscopy (SEM) (Mira 3 Tescan; Brno-Kohoutovice, Czech Republic). The freeze-dried samples were fixed to a metal stub using an adhesive tape and coated with the gold

layer before the observation with an electrical voltage of 5.0 kV and $25.0\text{k}\times$ magnifying power.

Carboxylic acid content

The amount of carboxylic acid group on the AA/VP PNPs was quantified using salt-splitting titration. Briefly, the PNPs (20 mg) were immersed in 0.01 N NaOH (25 mL) overnight. The excess NaOH was titrated with 0.0100 N HCl to the phenolphthalein endpoint, which was indicated by the conversion of a pink colored solution to a colorless one. The amount of carboxylic acid groups on the AA/VP PNPs was computed using eqn (1).

$$\text{Amount of COOH (mmol g}^{-1}\text{)} = \frac{(V_{\text{VR}} - V_{\text{t}}) \times C}{\text{weight of PNPs}} \quad (1)$$

where V_{VR} is the volumetric relation between the titrant and the titrand, V_{t} is the volume of titrant used to the endpoint of each sample, C is the standardized concentration of HCl.

Thiol content

Ellman's assay was conducted to determine the amount of thiol group grafted on the AA/VP NPs. Various concentrations of L-cysteine HCl were prepared in phosphate buffer saline (PBS) to obtain a standard curve ranging between $1\text{--}20\text{ }\mu\text{g mL}^{-1}$. Samples (1 mg mL^{-1}) dissolved in PBS were mixed with Ellman's reagent (0.3 mg mL^{-1}) at the volume ratio of 1 : 1, followed by a 2 h incubation in the dark. Then, an aliquot ($300\text{ }\mu\text{L}$) of the mixture was placed in each well of a 96-well plate, and the absorbance was measured in triplicate using a VICTOR Nivo™ multimode microplate reader (PerkinElmer, MA, USA) at 412 nm.

Ex vivo mucoadhesion

The mucoadhesive study of the synthesized PNPs was examined using the *ex vivo* flow-through method. Sodium fluorescein (NaFN) was loaded onto each sample by mixing NaFN with the PNPs (0.5 : 1 by weight) overnight using a rotator mixer. The fresh porcine buccal mucous membrane was excised into $10 \times 10\text{ mm}^2$ pieces and placed on a glass slide. A total of $20\text{ }\mu\text{L}$ of each fluorescence-loaded PNP was placed on the mucous membrane. Simulated saliva fluid (NaCl (8 g), KH_2PO_4 (0.19 g), and Na_2HPO_4 (2.38 g), and o-phosphoric acid to pH 6.8) was employed to rinse off the sample at the rate of 1 mL min^{-1} for 60 min. After each specified time, the mucosal sample was captured under a fluorescence stereomicroscope (Leica M60, Wetzlar, Germany), and the green fluorescence intensity (FI) at different time points (FI_t) was analyzed by the LAS X software v.3.6. The percentage of PNPs left on the membrane was calculated relative to the amount of pre-washing FI (FI_0) following eqn (2).

$$\% \text{ PNPs remained} = \frac{\text{FI}_t - \text{FI}_{\text{blank}}}{\text{FI}_0 - \text{FI}_{\text{blank}}} \times 100 \quad (2)$$

Nicotine loading

Nicotine was loaded onto the preactivated-thiolated AA/VP PNPs using the adsorption method. The preactivated-thiolated AA/VP PNPs were weighed and dispersed in deionized water at 0.5 mg mL^{-1} . The drug was added to the dispersion at different weight ratios of the PNPs to nicotine (1 : 1, 1 : 3, and 1 : 5) before shaking



overnight. After that, the samples were centrifuged at 4000 rpm for 15 min and washed thrice with deionized water before freeze drying to collect the nicotine-loaded preactivated-thiolated AA/VP PNPs. The dried samples were then accurately weighed and dissolved in glacial acetic acid. The amount of the nicotine was quantified by non-aqueous potentiometric titration using a standardized 0.0100 M perchloric acid as a titrant in accordance with the method described in the United States Pharmacopeia 43 (USP 43). The loading capacity (LC) and the percentage of loading efficiency (% LE) were calculated from eqn (3) and (4), respectively.

$$LC(\mu\text{g mg}^{-1}) = \frac{\text{amount of nicotine found}}{\text{weight of nicotine - loaded PNPs}} \quad (3)$$

$$\% \text{ LE} = \frac{\text{amount of nicotine found}}{\text{total amount of nicotine}} \times 100 \quad (4)$$

Drug release

The release of nicotine from the preactivated-thiolated AA/VP PNPs was determined using a dialysis technique. A total of 10 mg of the drug-loaded PNPs were weighed and dispersed homogeneously to form a colloidal dispersion in the dialysis bags (molecular weight cut-off: 6000–8000 Da). The bags were immersed in the simulated saliva (30 mL) and shaken at a constant rate in an incubator shaker ($37 \pm 0.5^\circ\text{C}$, 50 rpm). At the pre-determined times, the released medium (10 mL) was sampled and replaced with a fresh medium (10 mL) to maintain sink condition. The cumulative release of nicotine was analyzed by a UV-visible spectrophotometer (Cary 60 UV-Vis, Agilent Technologies, Santa Clara, CA, USA) at 260 nm.

Biocompatibility

The biocompatibility of the synthesized preactivated-thiolated AA/VP PNPs to the normal human gingival fibroblast (HGF) cell line was proven using MTT assay. The cells were cultivated in a complete Dulbecco's modified Eagle's medium (DMEM) (Gibco BRL, Rockville, MD, USA) and seeded to a 96-well plate (10 000 cells per well, 100 μL). The HGF cells were then incubated in an incubator (37°C , 5% CO_2 , and 95% air atmosphere) for 1 day. The blank preactivated-thiolated AA/VP PNPs were prepared in serum-free DMEM at various concentrations (0.1–1000 $\mu\text{g mL}^{-1}$) and placed in each well of a 96-well plate. Triton X-100 (1% v/v) was used as positive control. After 24 h treatment, the PNP solution was removed. Complete DMEM containing MTT (0.5 mg mL^{-1}) was then added to each well. Then, the well plate was kept in an incubator for another 3 h. The formazan crystals that formed were dissolved with dimethyl sulfoxide (DMSO). The absorbance was analyzed at 550 nm using a multimode microplate reader. The percentage of viable cells was calculated relative to the untreated control cells.

Statistical analysis

All experiments were performed in triplicate. Numerical data were reported as mean \pm standard deviation. The analysis of variance and comparisons were analyzed using 95% confidence

interval with *F*-test and independent *t*-test, respectively. The *p* < 0.05 states significant differences.

Results and discussion

Synthesis of AA/VP PNPs

The AA/VP PNPs were synthesized by surfactant-free emulsion polymerization reaction from two monomers (AA and VP), which was initiated with the AAPH free radical initiator. The structural attributes of the obtained PNPs were characterized using ^1H -NMR and ATR-FTIR. From the ^1H -NMR spectra (Fig. 2a), the protons of the polymerized $\text{CH}_2\text{-CH}_2$ core structure and C3 protons of the pyrrolidone ring were presented as

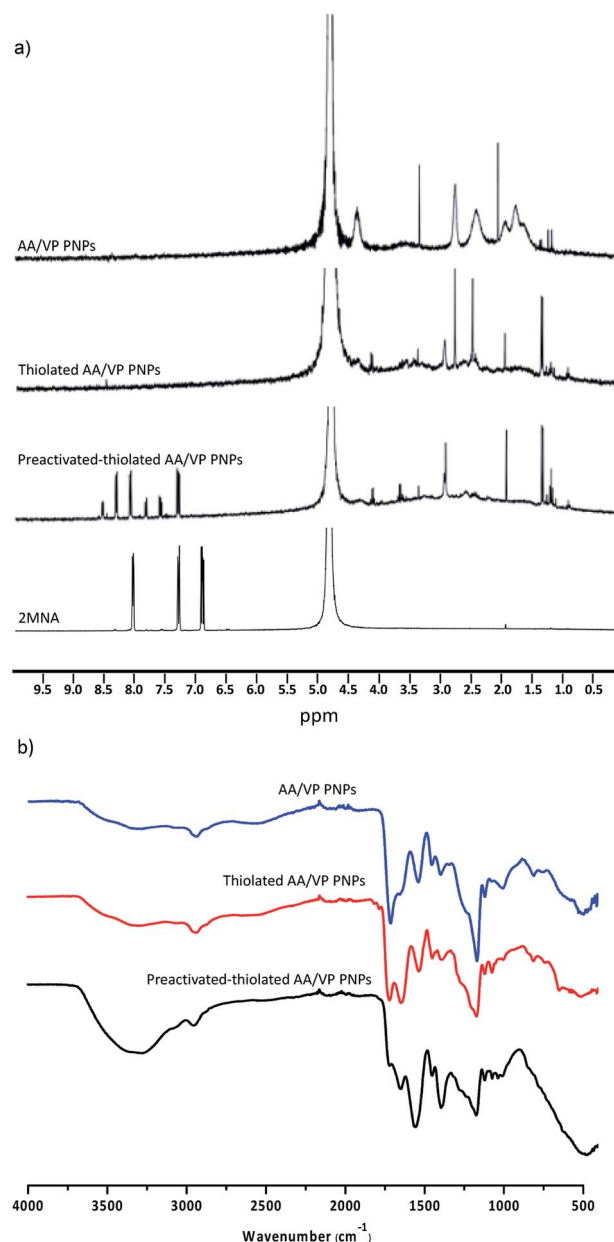


Fig. 2 Spectroscopic characterizations of the AA/VP PNPs, the thiolated AA/VP PNPs, and the preactivated-thiolated AA/VP PNPs: (a) ^1H -NMR spectra and (b) ATR-FTIR spectra.



Table 1 Characteristics of the synthesized PNPs

PNPs	Particle size (nm)	PDI	Zeta potential (mV)	Amount of COOH (mmol g ⁻¹)	Thiol content (μmol g ⁻¹)
AA/VP PNPs	268.3 ± 5.9	0.2 ± 0.0	-21.3 ± 0.3	6.7 ± 0.1	—
Thiolated AA/VP PNPs	300.7 ± 8.0	0.3 ± 0.0	-3.5 ± 0.4	—	607.6 ± 15.1
Preactivated-thiolated AA/VP PNPs	425.5 ± 29.7	0.3 ± 0.0	-33.3 ± 0.4	—	—

multiplets at 1.45–2.57 ppm. The protons of the carboxylic groups and C3 of the pyrrolidone ring were represented by a multiplet at 2.76 ppm. Another multiplet at 4.35 ppm referred to the protons of the core chain of the pyrrolidone ring. Fig. 2b presents the ATR-FTIR spectra of the AA/VP PNPs. The spectra showed the polymerized C–H stretching at 2924 cm⁻¹, and the broad O–H stretching of the AA hydroxyl appeared at 3316 cm⁻¹. The strong carboxylic carbonyl, C–O stretching, and carboxylate COO⁻ vibrations were represented by the peaks at 1704, 1161 and 1402 cm⁻¹, respectively. The C–N stretching at 1112 cm⁻¹ along with the cyclic amide (O=CN) band at 1641 cm⁻¹ corresponded to the pyrrolidone ring of the PNPs. The spectra of both spectrometric investigations confirmed the structure of the synthesized AA/VP PNPs.

Synthesis of thiolated AA/VP PNPs

The coupling reaction was operated to graft the thiol moiety from L-cysteine to the AA/VP PNPs. Spectroscopic investigations were performed to elucidate the structure of the SH-AA/VP PNPs. The ¹H-NMR spectrum of the thiolated AA/VP PNPs (Fig. 2a) revealed a splitting pattern corresponding to the spectrum of AA/VP PNPs. The protons of L-cysteine were presented as a doublet (2.78 ppm) and a triplet (4.15 ppm), which were attributed to the protons of β and α carbons, respectively. After conjugating the carboxylic acid groups of AA/VP PNPs with the primary amine of L-cysteine, the secondary aliphatic amide functional group was formed. Fig. 2b displays the FTIR spectrum of the thiolated AA/VP PNPs. The sharp band at 1642 cm⁻¹ referred to the secondary amide bond, whereas other stretchings and vibrations conformed to the spectrum of the AA/VP PNPs. The O–H stretching was broadened due to the hydrogen bond from the cysteine carboxyl groups at 3301 cm⁻¹. The ¹H-NMR and ATR-FTIR spectra assured the successful addition of thiol groups onto the PNPs.

Synthesis of preactivated-thiolated AA/VP PNPs

The thiol–disulfide exchange reaction was conducted to preactivate the thiol groups on the thiolated AA/VP PNPs. In this reaction, the DTNA dimers obtained from the oxidative coupling reaction of 2MNA monomers were electron deficient at the disulfide linkage. Therefore, the disulfide bond acted as an electrophile and exchanged its disulfide bond with the nucleophilic thiol group in the PNPs, resulting in the attachment of 2MNA to the thiolated AA/VP PNPs through the new disulfide bond. The structure of the preactivated thiolated AA/VP PNPs was characterized by ¹H-NMR and ATR-FTIR. From the

spectrum of the preactivated PNPs shown in Fig. 2a, the major peaks of the preactivated thiolated AA/VP PNPs were similar to those of AA/VP PNPs and thiolated AA/VP PNPs. However, the splitting of 2MNA at the outer shell of the preactivated thiolated AA/VP PNPs was observed in the spectrum. After disulfide formation, signals of 2MNA shifted to the downfield region as a result of the deshielding effect. The C4 proton of the conjugated pyridine ring of 2MNA was presented as doublets at 7.84 and 8.09 ppm, the C5 proton was shown as multiplets at 7.31 and 7.61 ppm, and the C6 proton was displayed as doublets at 8.33 and 8.55 ppm. Although the chemical shifts of the preactivated 2MNA differed from that of pure 2MNA, the coupling constant of each proton correlates to the free 2MNA signals (C4–C6 H, *J* = 3.1, 4.5, 2.3 Hz, respectively). These results indicate the completion of PNP preactivation. Fig. 2b displays the ATR-FTIR spectrum of the preactivated PNPs. The spectrum exhibited signals corresponding to the AA/VP PNP and thiolated AA/VP PNP spectra. Nevertheless, the spectra of the preactivated thiolated AA/VP PNPs presented a broad and intensified O–H stretching at 3307 cm⁻¹ due to the addition of a carboxylic acid group. Moreover, the C=C stretching of the pyridine ring was displayed at 1549 cm⁻¹, demonstrating the successful attachment of 2MNA to the preactivated thiolated AA/VP PNPs.

Characterizations of the PNPs

The particle size and surface charge of the synthesized PNPs were characterized by dynamic light scattering (DLS). Table 1 discloses that the size of the AA/VPs PNPs was less than 300 nm with a narrow size distribution. The negative surface charge of the PNPs was due to the carboxylic group of AA. The amount of COOH on the AA/VP PNPs was 6.7 ± 0.1 mmol g⁻¹, which was used as guide for determining the amount of cysteine to be added in the synthesis reaction of thiolated AA/VP PNPs. After the thiolation of PNPs, their particle size grew significantly because of the complex chemical structure of thiolated AA/VP PNPs. However, the size failed to achieve a high polydispersity index. The zeta potential of the thiolated PNPs remained negative, but the value dropped, which possibly resulted from the protonation of conjugated L-cysteine.^{30,31} The thiol content of PNPs preferably enhanced the mucoadhesive property of the PNPs. After preactivation, the size of preactivated thiolated AA/VP PNPs was notably larger than their previous version because the structure of the latter was more complicated. The surface charge of the preactivated thiolated AA/VP PNPs was just above -30 mV, which can prevent particle aggregation through electrostatic repulsion.^{32,33} Furthermore, the morphology of the synthesized preactivated thiolated AA/VP PNPs was preferably



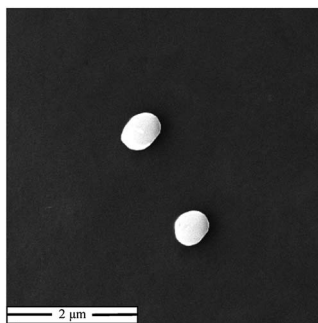


Fig. 3 SEM photograph of the synthesized preactivated-thiolated AA/VP PNPs (at 25.0k \times magnification).

spherical, as observed by SEM (Fig. 3), with the size conforming to the information provided by DLS. These investigations suggest that PNPs can be a candidate for transmucosal drug delivery.³⁴

Ex vivo mucoadhesion

The mucoadhesive capability of the preactivated thiolated AA/VP PNPs was determined by a flow-through mucoadhesion test. The amount of PNPs that remained on the porcine buccal membrane after rinsing was determined compared with the thiolated AA/VP PNPs and dextran, which were used as controls. The amount of the PNPs retained on the mucous membrane

was analyzed by measuring the FI under a fluorescence stereo-microscope relative to the initial FI. The finding was reported as a percentage of the PNPs remained (Fig. 4a). As observed from the results, dextran (nonadhesive polymer) was washed out immediately after being washed with 5 mL artificial saliva, and 20% of the initial amount was retained on the tissue after washing for 60 min. On the other hand, the thiolated AA/VP PNPs firmly adhered to the mucosal membrane with almost 40% left on the tissue after 1 h washing. Interestingly, the preactivated thiolated AA/VP PNPs attached to the mucosa with a significantly higher amount than the thiolated AA/VP PNPs and dextran, with less than 20% of the PNPs on the tissue rinsed off in 5 min, and approximately 60% remained on the tissue at the end of the experiment. Fig. 4b displays the images presenting the FI of the remaining PNPs on the mucosa. The images pointed out that the adhesions of the preactivated thiolated AA/VP PNPs were superior to those of thiolated AA/VP PNPs and dextran. The fluorescence of NaFN-loaded dextran significantly faded at the earliest time point, whereas both PNPs fade slowly over time. Thiolated polymers and nanocarriers are a potent mucoadhesive platform in various mucosal surfaces.^{19,35} The formation of a covalent disulfide bridge between the thiols of the thiolated AA/VP PNPs and those of cysteine residues in the mucin glycoprotein may be involved in the mucoadhesive capability of the thiolated AA/VP PNPs.³⁶ The bond formation is irreversible and can provide a prolonged and robust mucoadhesion. However, the thiol moieties were

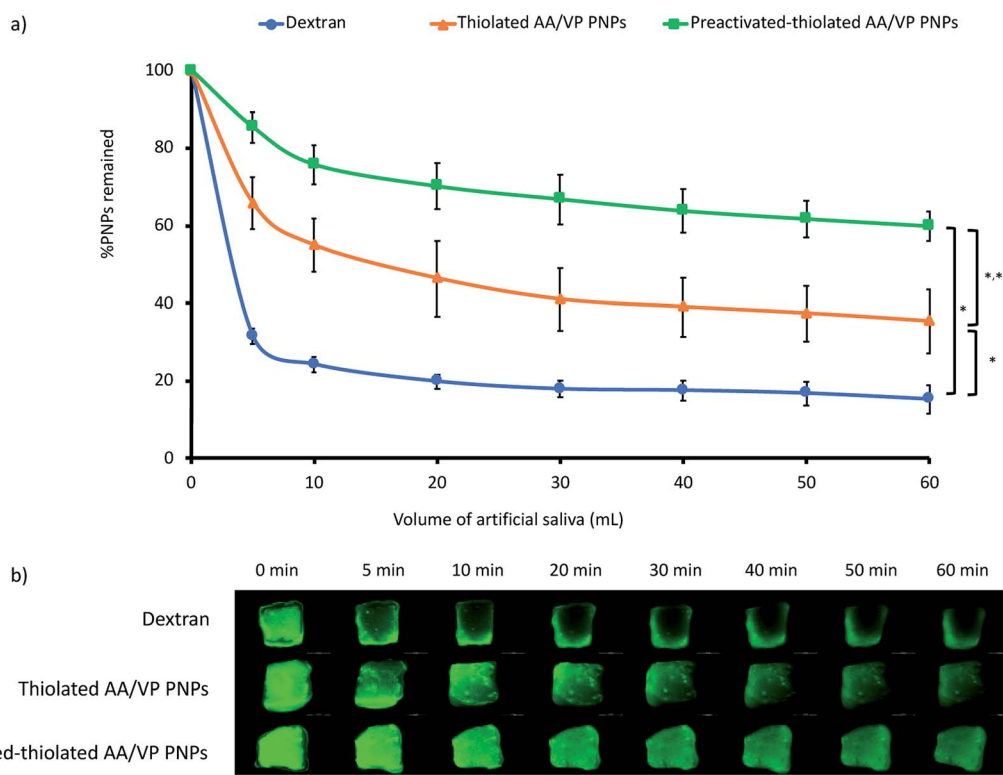


Fig. 4 The mucoadhesive property of the preactivated-thiolated AA/VP PNPs compared to the thiolated AA/VP PNPs and dextran: (a) percentage remaining after being washed off by artificial saliva, (b) fluorescent intensity of the NaFN-loaded PNPs or dextran on the porcine buccal mucosa after being washed off by artificial saliva (*significant difference at the final timepoint ($p < 0.05$)).



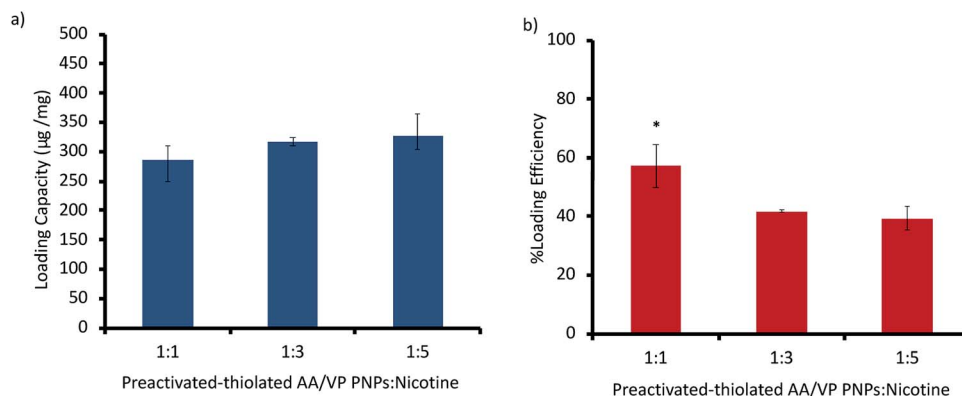


Fig. 5 (a) Loading capacity and (b) % loading efficiency of nicotine onto the preactivated-thiolated AA/VP PNPs at different PNPs : nicotine ratios. *Significant different from other ratios ($p < 0.05$).

unstable and readily active for oxidation, leading to less thiol group attachment to the glycoprotein.^{20,21} Preactivated thiomers may solve the stability concerns of thiomers by preventing thiol oxidation during storage. Preactivation forms a disulfide linkage between the thiol of the mucoadhesive polymer and that of an electron-deficient leaving group. The thiol-disulfide exchange spontaneously occurs in a physiological condition to trigger the mucoadhesive phenomenon. In addition, the preactivation of thiol groups enhances the reactivity of the moiety to interact with cysteine thiol.³⁷ Preactivated thiols can firmly adhere to the mucous membrane and consequently enhance the adhesion of mucoadhesive platforms. Hence, the preactivated thiolated AA/VP PNPs facilitated mucoadhesion on the porcine buccal membrane at a high quality compared with non-preactivated PNPs.

Nicotine loading and release

Nicotine was incorporated into the preactivated thiolated AA/VP PNPs through an adsorption procedure. The protonated nicotine at a neutral pH condition can form ionic interactions along with hydrogen bonds with negatively charged PNPs. The optimal drug loading parameter was determined from the LC and % LE (Fig. 5a and b, respectively). The LC of nicotine on the preactivated thiolated AA/VP PNPs were in the range of 285–326 $\mu\text{g}/\text{mg}$ in all ratios ($p > 0.05$). However, % LE was significantly higher at the PNPs : nicotine ratio of 1 : 1 (60%) compared with the other ratios ($p < 0.05$). Increasing the amount of the drug did not increase the drug loading. This finding may be because the PNPs has reached their highest capability, and the drug could no longer adsorb onto the PNPs beyond the PNP : nicotine ratio of 1 : 1. Given LC and % LE, the PNP : nicotine ratio of 1 : 1 was therefore selected for further investigations.

The release of nicotine from preactivated thiolated AA/VP PNPs was investigated by the dialysis technique. At each time point, the release medium was collected, and the amount of nicotine was determined using a UV spectrophotometer set at 260 nm. The biphasic release of nicotine from the preactivated PNPs was observed (Fig. 6). Almost 50% of nicotine in the PNPs was released in 1 h followed by a gradual release of up to 87% in

12 h. The burst release of the drug at the initial period possibly resulted from the nicotine adsorption at the outer surfaces of the PNPs, which can provide the rapid action of the formulation. The swelling of hydrophilic PNPs then influenced the dissolution of the drug and sustained the nicotine release in the following phase. The prolonged-release period of up to 12 h demonstrated the potential of mucoadhesive PNPs to extend the delivery of nicotine in the oral cavity and ascertain nicotine delivery throughout administration. This drug release behavior may be beneficial to prolong the active compound in the body compared with the orally given commercial nicotine gums which need frequent daily dosing to avoid nicotine withdrawal symptoms. Although the release of nicotine from the developed carrier showed a burst release for approximately 70% in the first 2 h due to the hydrophilic nature of nicotine, the characteristic can be beneficial compared with the commercial nicotine gum which is a commonly used formulation. The nicotine gum can reach its maximum plasma concentration within 15–30 min after the administration. Hence, the burst release of the formulated nicotine-loaded mucoadhesive PNPs can deliver a loading dose of nicotine and be advantageous to prevent patients' craving at the initial phase. Meanwhile, the sustained release profile can further deliver nicotine to extend nicotine plasma concentration in place of the eliminated drug (half-life:

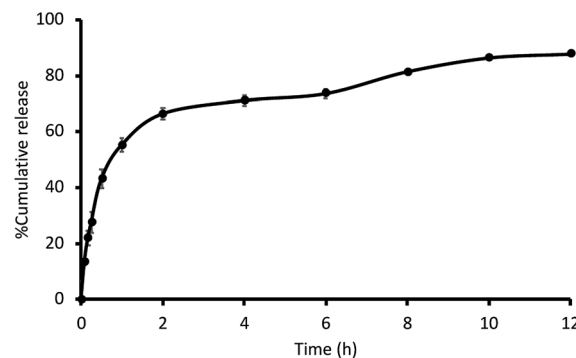


Fig. 6 The release characteristics of nicotine from the 2MNA-SH-AA/VP PNPs in artificial saliva.

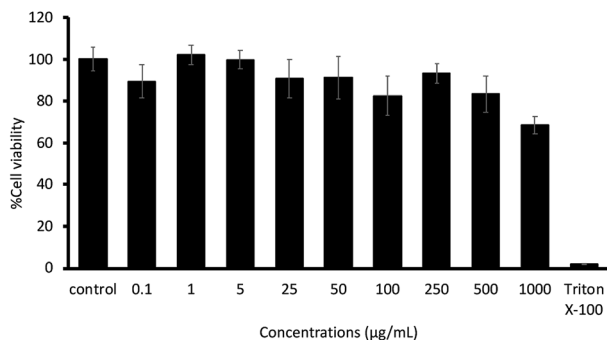


Fig. 7 The cytotoxicity of the preactivated-thiolated AA/VP PNPs on HGF cells.

1.6–2.8 h). This condition will assist the reduction of the dosing frequency. We suggest that the biphasic delivery of nicotine can be advantageous compared with the commercial nicotine gum, in which a second dose may be necessary several hours after the initial administration.^{11,38,39} For the retarded release of nicotine, adding a hydrophobic monomer to the PNP synthesis would result in a slow release profile.

Biocompatibility of the preactivated-thiolated AA/VP PNPs

The biocompatibility of the synthesized preactivated thiolated AA/VP PNPs was determined by MTT assay. Fig. 7 exhibits the percentage of relative cell viability. The results revealed that relative to the untreated cells (control), the synthesized mucoadhesive PNPs were nontoxic to the HGF cells under the duration and concentrations studied, whereas the positive control (1% v/v Triton X-100) showed a significant cell lysis. This finding may be because the monomers involved in the synthesis of the PNPs were safe to the human body at the appropriate concentration. However, further *in vivo* examinations are necessary to demonstrate the irritability and toxicity of preactivated thiolated AA/VP PNPs.

Conclusions

Preactivated thiolated AA/VP PNPs have been developed by synthesizing AA/VP PNPs *via* emulsion polymerization, followed by thiolation with L-cysteine and preactivation with 2MNA. The nano-size PNPs were spherical and had a negative surface charge. The preactivated thiolated AA/VP PNPs were expected to prevent the oxidation of the thiol moiety and enhanced sensitivity of thiol–disulfide reaction to adhere to the mucin glycoprotein. The mucoadhesive property of the preactivated PNPs was superior to that of thiolated PNPs. Nicotine was preferably adsorbed onto the preactivated thiolated AA/VP PNPs with biphasic release characteristics. The rapid release followed by a sustained release of nicotine from the PNPs can provide the rapid relief of cigarette craving symptoms and avoid nicotine withdrawal symptoms. Furthermore, the synthesized mucoadhesive PNPs were nontoxic to the HGF cells. Therefore, the development of nicotine-loaded mucoadhesive preactivated

thiolated AA/VP PNPs as a nicotine replacement formulation illustrates a potential future candidate for smoking cessation.

Conflicts of interest

The authors declared no conflicts of interest.

Acknowledgements

The authors would like to acknowledge the financial support from the Thailand Research Funds through the Research Team Promotion Grant (RTA 6180003) and through the Golden Jubilee PhD Program (Grant No. PHD/0021/2560). Furthermore, we would like to thank Mr Akira Patthaisong, Mr Alonggorn Kuisorn, and Mr Pittawas Jentrakulroj for their dedication as research assistants to complete the research.

References

- 1 M. A. Chandler and S. I. Rennard, in *Asthma and COPD*, ed. P. J. Barnes, J. M. Drazen, S. I. Rennard and N. C. Thomson, Academic Press, Oxford, 2nd edn, 2009, pp. 599–607, DOI: 10.1016/B978-0-12-374001-4.00047-X.
- 2 N. L. Benowitz, *N. Engl. J. Med.*, 2010, **362**, 2295–2303.
- 3 I. McLaughlin, J. A. Dani and M. De Biasi, *Curr. Top. Behav. Neurosci.*, 2015, **24**, 99–123.
- 4 A. Pipe, in *Cardiology Secrets*, ed. G. N. Levine, Elsevier, 5th edn, 2018, pp. 394–398, DOI: 10.1016/B978-0-323-47870-0.00044-1.
- 5 R. S. Barua, N. A. Rigotti, N. L. Benowitz, K. M. Cummings, M.-A. Jazayeri, P. B. Morris, E. V. Ratchford, L. Sarna, E. C. Stecker and B. S. Wiggins, *J. Am. Coll. Cardiol.*, 2018, **72**, 3332.
- 6 M. Verbiest, E. Brakema, R. van der Kleij, K. Sheals, G. Allistone, S. Williams, A. McEwen and N. Chavannes, *NPJ Prim. Care Respir. Med.*, 2017, **27**, 2.
- 7 A. Batra, *Dtsch. Arztebl. Int.*, 2011, **108**, 555–564.
- 8 J. E. Henningfield, R. V. Fant, A. R. Buchhalter and M. L. Stitzer, *Ca-Cancer J. Clin.*, 2005, **55**, 281–299; quiz 322–283, 325.
- 9 U. Wadgave and L. Nagesh, *Int. J. Health Sci.*, 2016, **10**, 425–435.
- 10 J. T. Hays, in *Cardiology Secrets*, ed. G. N. Levine, Mosby, Philadelphia, 3rd edn, 2010, pp. 305–310, DOI: 10.1016/B978-032304525-4.00047-2.
- 11 L. Shahab, L. S. Brose and R. West, *CNS Drugs*, 2013, **27**, 1007–1019.
- 12 T. Pongjanyakul, W. Khunawattanakul, C. J. Strachan, K. C. Gordon, S. Puttipipatkachorn and T. Rades, *Int. J. Biol. Macromol.*, 2013, **55**, 24–31.
- 13 O. C. Okeke and J. S. Boateng, *Carbohydr. Polym.*, 2017, **155**, 78–88.
- 14 J. Boateng and O. Okeke, *Pharmaceutics*, 2019, **11**, 104.
- 15 S. Mansuri, P. Kesharwani, K. Jain, R. K. Tekade and N. K. Jain, *React. Funct. Polym.*, 2016, **100**, 151–172.
- 16 S. Roy, K. Pal, A. Anis, K. Pramanik and B. Prabhakar, *Des. Monomers Polym.*, 2009, **12**, 483–495.



- 17 P. Abhang, M. Momin, M. Inamdar and S. Kar, *Drug Deliv. Lett.*, 2014, **4**, 26–37.
- 18 S. Duggan, W. Cummins, O. O' Donovan, H. Hughes and E. Owens, *Eur. J. Pharm. Sci.*, 2017, **100**, 64–78.
- 19 M. Hanif, M. Zaman and S. Qureshi, *Int. J. Polym. Sci.*, 2015, **2015**, 1–9.
- 20 J. Iqbal, G. Shahnaz, S. Dunnhaupt, C. Muller, F. Hintzen and A. Bernkop-Schnurch, *Biomaterials*, 2012, **33**, 1528–1535.
- 21 I. Pereira de Sousa, W. Suchaoain, O. Zupancic, C. Lechner and A. Bernkop-Schnurch, *Carbohydr. Polym.*, 2016, **152**, 632–638.
- 22 E. Calzoni, A. Cesaretti, A. Polchi, A. Di Michele, B. Tancini and C. Emiliani, *J. Funct. Biomater.*, 2019, **10**, 4.
- 23 K. M. El-Say and H. S. El-Sawy, *Int. J. Pharm.*, 2017, **528**, 675–691.
- 24 C. Pornpitchanarong, T. Rojanarata, P. Opanasopit, P. Patrojanasophon and T. Ngawhirunpat, *MATEC Web Conf.*, 2018, **192**, 01020.
- 25 K. M. Koczkur, S. Mourdikoudis, L. Polavarapu and S. E. Skrabalak, *Dalton Trans.*, 2015, **44**, 17883–17905.
- 26 Y. Hu, X. Jiang, Y. Ding, H. Ge, Y. Yuan and C. Yang, *Biomaterials*, 2002, **23**, 3193–3201.
- 27 R. M. Molnar, M. Bodnar, J. F. Hartmann and B. Janos, *Colloid Polym. Sci.*, 2009, **287**, 739–744.
- 28 C. Pornpitchanarong, T. Rojanarata, P. Opanasopit, T. Ngawhirunpat and P. Patrojanasophon, *Colloids Surf., B*, 2020, **185**, 110566.
- 29 M. Perrone, A. Lopalco, A. Lopedota, A. Cutrignelli, V. Laquintana, J. Douglas, M. Franco, E. Liberati, V. Russo, S. Tongiani, N. Denora and A. Bernkop-Schnurch, *Eur. J. Pharm. Biopharm.*, 2017, **119**, 161–169.
- 30 J. Morgan, A. Greenberg and J. F. Liebman, *Struct. Chem.*, 2012, **23**, 197–199.
- 31 M. Szostak, L. Yao, V. W. Day, D. R. Powell and J. Aubé, *J. Am. Chem. Soc.*, 2010, **132**, 8836–8837.
- 32 E. Joseph and G. Singhvi, in *Nanomaterials for Drug Delivery and Therapy*, ed. A. M. Grumezescu, William Andrew Publishing, 2019, pp. 91–116, DOI: 10.1016/B978-0-12-816505-8.00007-2.
- 33 A. Kumar and C. K. Dixit, in *Advances in Nanomedicine for the Delivery of Therapeutic Nucleic Acids*, ed. S. Nimesh, R. Chandra and N. Gupta, Woodhead Publishing, 2017, pp. 43–58, DOI: 10.1016/B978-0-08-100557-6.00003-1.
- 34 S. Hua, *Front. Pharmacol.*, 2019, **10**, 1328.
- 35 K. Albrecht and A. Bernkop-Schnurch, *Nanomedicine*, 2007, **2**, 41–50.
- 36 S. Yuan, M. Hollinger, M. E. Lachowicz-Scroggins, S. C. Kerr, E. M. Dunican, B. M. Daniel, S. Ghosh, S. C. Erzurum, B. Willard, S. L. Hazen, X. Huang, S. D. Carrington, S. Oscarson and J. V. Fahy, *Sci. Transl. Med.*, 2015, **7**, 276ra27.
- 37 S. Hauptstein, S. Dezorzi, F. Prufert, B. Matuszczak and A. Bernkop-Schnurch, *Carbohydr. Polym.*, 2015, **124**, 1–7.
- 38 A. C. Holloway, in *Encyclopedia of Toxicology*, ed. P. Wexler, Academic Press, Oxford, 3rd edn, 2014, pp. 514–516, DOI: 10.1016/B978-0-12-386454-3.00521-2.
- 39 A. I. Herman and M. Sofuoglu, in *Interventions for Addiction*, ed. P. M. Miller, Academic Press, San Diego, 2013, pp. 337–343, DOI: 10.1016/B978-0-12-398338-1.00035-X.

